Proceedings of the 7th International Conference on HydroScience and Engineering

Philadelphia, USA September 10-13, 2006 (ICHE 2006)
ISBN: 0977447405

Drexel University
College of Engineering

Drexel E-Repository and Archive (iDEA)
http://idea.library.drexel.edu/

Drexel University Libraries
www.library.drexel.edu

Please direct questions to archives@drexel.edu

THREE-DIMENSIONAL HYDRODYNAMIC MODELING
OF SAN PABLO BAY ON AN UNSTRUCTURED GRID

Michael L. MacWilliams[1] and Ralph T. Cheng[2]

ABSTRACT

A three-dimensional hydrodynamic model of San Francisco Bay was developed using the three-dimensional hydrodynamic model UnTRIM. The model was calibrated using continuous water level measurements and ADCP data in San Francisco Bay, and validated during an additional simulation period using current velocity measurements. The model was developed to support the Hamilton Wetlands Restoration Project, a joint undertaking by the U.S. Army Corps of Engineers and the California Coastal Conservancy to restore 2.6 km^2 of tidal marsh bordering San Pablo Bay. The restoration effort is expected to make use of more than 8.1 million m^3 of dredged materials to raise the elevation of subsided wetlands. The placement of an Aquatic Transfer Facility (ATF) in San Pablo Bay is being considered by the U. S. Army Corps of Engineers to serve as a temporary holding site for dredge sediments before they are transferred to the Hamilton Wetlands restoration site. The San Francisco Bay model presented in this paper was developed as part of a larger study to evaluate potential impacts of the proposed ATF on circulation and sediment transport dynamics in San Pablo Bay. This paper presents the model calibration and validation, while the full analysis of proposed ATF conditions is presented in a separate technical report.

1.   INTRODUCTION

A three-dimensional hydrodynamic model of San Francisco Bay was developed as part of the Hamilton Wetlands Restoration Project, a joint undertaking by the U.S. Army Corps of Engineers and the California Coastal Conservancy. It is estimated that 85 to 90 percent of the historic tidal marshes bordering San Francisco Bay have been filled or significantly altered over the past two centuries (SBSP, 2006). The Hamilton Wetlands Restoration Project is part of a growing effort to restore a portion of these former marshes to tidal action. The Hamilton Wetlands Restoration site, historically dominated by tidal salt marsh habitat, was converted first to agricultural and then for use as the Hamilton Army Airfield (USACE, 1988). Since the site was originally diked, it has subsided six to nine feed below mean sea level, and more than 8.1 million m^3 of dredged materials are expected to be used to raise the elevation of these subsided wetlands (USACE, 1988). In order to facilitate the transfer of dredged material to the project site, and Aquatic Transfer Facility (ATF) is being considered by the U.S. Army Corps of Engineers to serve as a temporary holding site for dredge sediments before they are transferred to the Hamilton Wetlands Restoration site. The basic concept of the ATF consists of an excavated basin located in relatively deep water which can be

[1] Environmental Consultant, P.O. Box 225174, San Francisco, CA 94122-5174, USA (michael@rivermodeling.com)
[2] Project Chief, Estuarine Hydrodynamics, U.S. Geological Survey, Menlo Park, CA 94025 (rtcheng@usgs.gov)

used for temporary storage of dredge sediments. Dredged sediment is deposited in the basin under existing dredging operations and can then be removed from the ATF using a cutterhead dredge and transported to shore as it is needed for the Hamilton Wetlands Restoration Project site as it is needed for restoration efforts. The UnTRIM model of San Francisco Bay was used to evaluate potential ATF configurations and locations and to assess the potential impacts of the ATF on hydrodynamics in San Pablo Bay. This paper presents the methods, calibration, and validation for the San Francisco Bay model developed as part of this effort. The model calibration and validation focus on the area in San Pablo Bay near the Hamilton Restoration site, where the ATF is likely to be located. The subsequent analysis of proposed ATF conditions is presented in a separate technical report as part of the ongoing Hamilton Wetlands Restoration Project.

2.   METHODS

The primary tool used in this technical study was the three-dimensional hydrodynamic model UnTRIM (Casulli and Zanolli, 2005). A full description of the governing equations and numerical discretization are described in Casulli and Zanolli (2002, 2005). Additional aspects of the model formulation and development can be found in Casulli (1999) and Casulli and Walters (2000). The UnTRIM model solves the three-dimensional Navier-Stokes equations on an unstructured grid in the horizontal plane. The boundaries between vertical layers are at fixed elevations, and cell heights can be varied vertically to provide increased resolution near the surface or other vertical locations. Volume conservation is satisfied by a volume integration of the incompressible continuity equation, and the free-surface is calculated by integrating the continuity equation over the depth, and using a kinematic condition at the free-surface as described in Casulli (1990). The governing equations are discretized using a finite difference – finite volume algorithm. The numerical method allows full wetting and drying of cells in the vertical and horizontal directions. All details and properties of this state-of-the-art three-dimensional model are well-documented in peer reviewed literature (Casulli and Zanolli, 2002; 2005).

The TRIM3D model (Casulli and Cheng, 1992) and UnTRIM model have been applied previously to San Francisco Bay (Cheng and Casulli, 2002). The TRIM3D model (Casulli & Cattani 1994) which follows a similar numerical approach on structured horizontal grids has been widely applied in San Francisco Bay (e.g., Cheng et al. 1993; Cheng and Casulli, 1996; Gross et al., 1999; Gross and Schaaf & Wheeler 2003; Gross et al., 2006), and a 2D version, TRIM2D, is used in San Francisco Bay Physical Oceanographic Real-Time System, SFPORTS (http://sfports.wr.usgs.gov/sfports) (Cheng and Smith, 1998). Thus, the UnTRIM numerical approach has been well-tested in the San Francisco Estuary.

2.1   Input and Boundary Conditions

This project makes use of the already established UnTRIM model of San Francisco Bay (Cheng and Casulli, 2002), with additional grid refinement added in San Pablo Bay near the ATF project area. The model domain extends from the Pacific Ocean west of the Golden Gate to the western end of the Sacramento-San Joaquin Delta, and includes South Bay, Central Bay, San Pablo Bay, and Suisun Bay (Figure 1). The primary bathymetry data source for the model grid of South San Francisco Bay, Central Bay, and San Pablo Bay was NOAA DEM (Digital Elevation Model) data. The DEM data specifies depth on a 30 meter grid in San Francisco Bay. The DEM data were compiled by NOAA (National Oceanographic & Atmospheric Administration) using soundings and other bathymetry data collected in San Francisco Bay from 1979 to 1985. Coastal ocean bathymetry
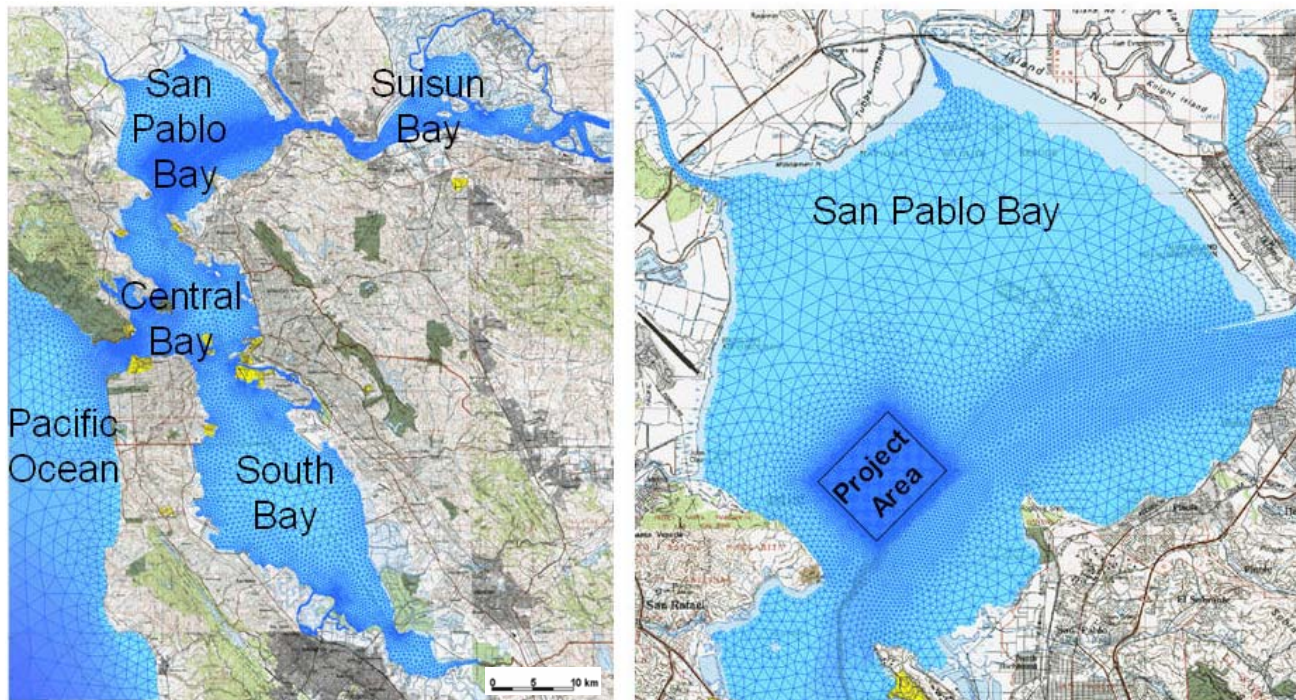
Figure 1 Model domain and grid for UnTRIM application to San Francisco Bay. The right panel
shows the details of grid distribution near the project area in San Pablo Bay.

was also derived from NOAA sounding data. In Suisun Bay the bathymetry was developed using
the USGS 10 m horizontal resolution bathymetric grid based on nearly one million depth soundings
augmented by contours and recent aerial photography (Smith et al., 2003). Each of the bathymetric
data sets was projected to the UTM NAD27 coordinate system and the vertical datum was adjusted
to NGVD29. A master bathymetric grid was developed from the combined data sources at a
resolution of 10 m. The bathymetric data was sampled at each grid node and the depth specified at
each grid face was set to be the average of the two nodes on each face.

The UnTRIM application to the Hamilton Wetland Restoration Project takes advantage of the grid
flexibility allowed in an unstructured mesh by incorporating a high resolution grid in the project
area, while using lower resolutions away from the project site. In the project area, a regular grid
consisting of 25 m by 25 m square grid cells was used in a 3 km by 3.5 km region where all of the
potential ATF sites are located. The total model grid is comprised of 53,552 horizontal grid cells
with 1 m vertical resolution, resulting in 578,000 three-dimensional cells. The grid is constructed
such that 64% of the horizontal grid cells are located within San Pablo Bay and 31% (16,800 cells)
are located within the highly refined 25 m uniform structured grid in the project area (Figure 1).
This approach allows for a detailed analysis of local hydrodynamics at the ATF site in San Pablo
Bay, while still incorporating the overall hydrodynamics of the larger estuary in a single model grid.

The model was forced using observed water levels at both the Pacific Ocean boundary and at the
upstream end of the model domain near Antioch, CA (located near the upstream extent of the model
domain on the top right of the left panel of Figure 1), following the approach used by SFPORTS
(Cheng and Smith, 1998). The ocean boundary was specified using observed water levels at the
NOAA station at Point Reyes (9415020), and the upstream boundary was specified using observed
water levels at the USGS water quality monitoring station at Antioch. Salinity at the ocean
boundary was assumed to be constant at 33.5 psu and salinity at the upstream boundary was
assumed to be 0 psu.

The bottom roughness height, z_o, is used to characterize the bottom friction. The specified z_o values varied as a function of water column depth and ranged from 0.1 mm to 2 mm, with the highest values in intertidal regions and the lowest values in the deep channel following the approach used by Gross et al. (2006). Because salinity calibration was not performed, a relatively simple algebraic vertical turbulence closure based on mixing length was used and freshwater inflows and evaporation were not included in the simulations. Similarly, because the study focused on currents in relatively deep areas wind effects and wind wave effects were not included in the hydrodynamic model.

3.   MODEL CALIBRATION

The model calibration period was selected based on available data for model calibration. The month of June was selected because June is a month with strong spring tides, and therefore produces stronger than average tidal currents in the project area. The model calibration focuses on water levels in San Francisco Bay at five locations along the axis of North San Francisco Bay and at an Acoustic Doppler Current Profiler (ADCP) located near Richmond (Figure 2). The primary sources of calibration data are shown Table 1. Because salinity calibration was not performed, a relatively short two-day period was sufficient to allow for spin-up of hydrodynamics prior to the calibration period.
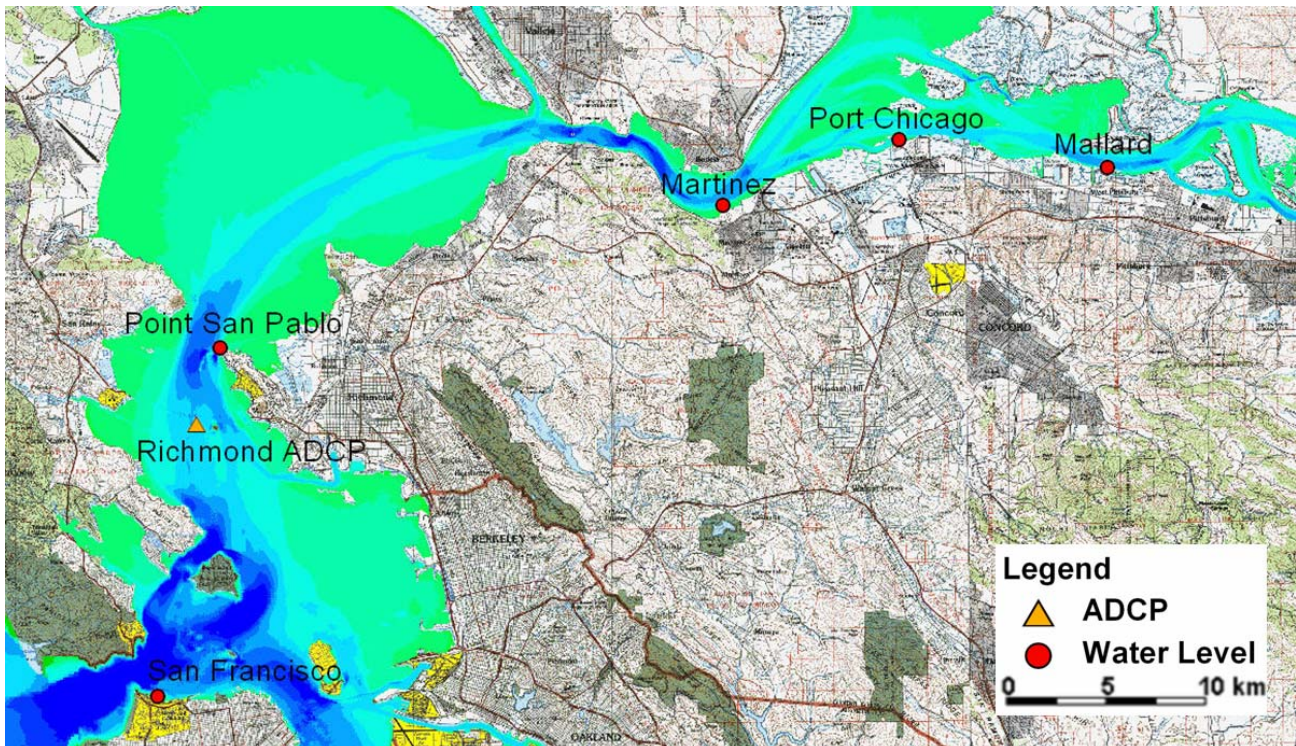

Figure 2 Hydrodynamic data stations for the 1998 calibration period.

Table 1 Model calibration data sources.

Location	Data Type	Data Source	Validation Record Length
San Francisco (9414290)	Water Level	NOAA	6/1/1998 – 7/1/1998
Point San Pablo	Water Level	USGS	6/1/1998 – 7/1/1998
Martinez	Water Level	USGS	6/1/1998 – 7/1/1998
Port Chicago (9415144)	Water Level	NOAA	6/1/1998 – 7/1/1998
Mallard Island	Water Level	USGS	6/1/1998 – 7/1/1998
Richmond	ADCP	USGS	6/1/1998 – 7/1/1998

Predicted and observed water levels at the San Francisco NOAA station at Fort Point (9414290) are shown in Figure 3a. As seen in this figure the predicted and observed water levels show very good agreement, nearly identical variations are shown with only very slight differences near high and low water at neap (weaker) tides. This demonstrates that the ocean boundary condition is accurately specified and is accurately propagating tides into San Francisco Bay. Predicted and observed water levels at the USGS continuous monitoring station at Point San Pablo are shown in Figure 3b. As seen in this figure, the predicted water levels show good agreement with observed water levels, both in terms of phase and tidal range, but the model tends to slightly under predict tidal range during neap tides and predicts slightly higher than observed water levels near low water during the second half of the validation period. At the USGS Martinez continuous monitoring station, the model shows a similar trend, with slightly less predicted tidal range for neap tides and again a small over-prediction of water surface elevations near low water (Figure 3c). At the NOAA station at Port Chicago (9415144) the model shows very good agreement with observed water levels both in terms of phase and tidal range (Figure 3d). The observed and predicted water levels at the USGS Mallard Island continuous monitoring station (Figure 3e) also show very good agreement, indicating that the boundary condition at Antioch is properly forcing water levels near the upstream end of the model domain.
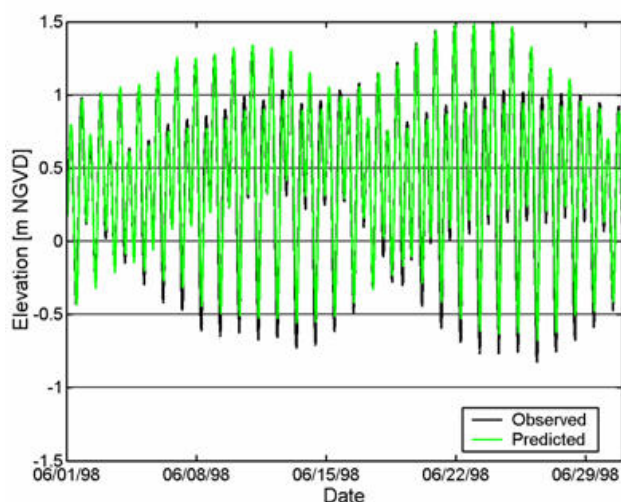
The observed and predicted depth-averaged current speed and direction at the Richmond ADCP (location on Figure 2) are shown on Figure 3f. The model accurately predicts phase and direction of tidal currents throughout the analysis period.   The predicted current speed shows very good agreement with observed current speed during the first and third weeks of the simulation period, while the model tends to under predict peak ebb current speeds during the second and fourth week of the simulation. The predicted current speeds show similar trends to the observed current speeds both in terms of spring-neap variability and semi-diurnal variability of current speeds.   Overall the level of agreement between the observed and predicted current speeds is good, except for peak current speeds during spring tides when the model tends to under predict peak ebb currents. The observed and predicted current speed at the Richmond ADCP on June 24, 1998 during relatively strong spring tides is shown on Figure 4. On June 24, the model shows very good agreement at the Richmond ADCP both in terms of current speed and direction. The model under predicts the first ebb current speed peak by 15% or approximately 20 cm/s but shows better agreement with both flood current speed peaks and the weaker ebb current speed peak. The current direction during each of the tidal phases shows very good agreement with observed direction.
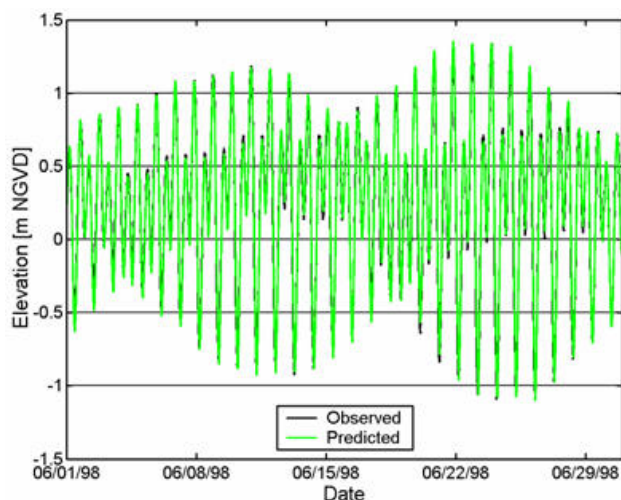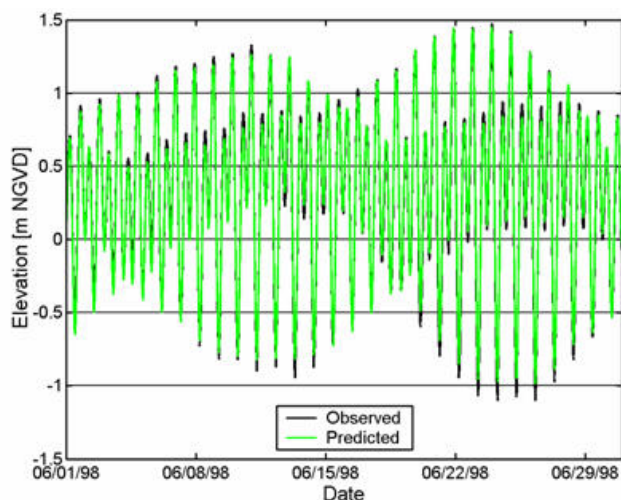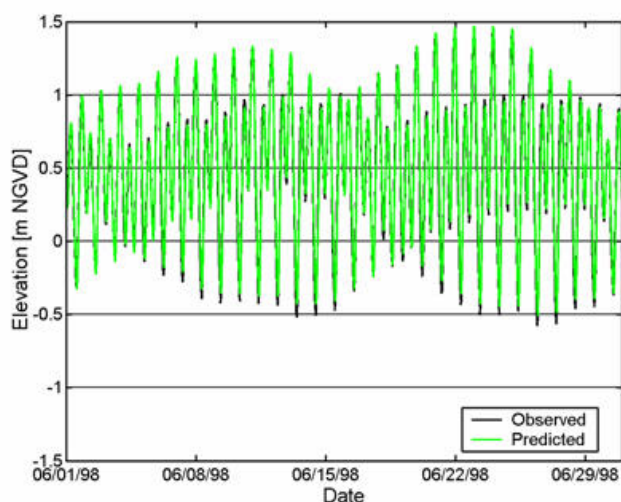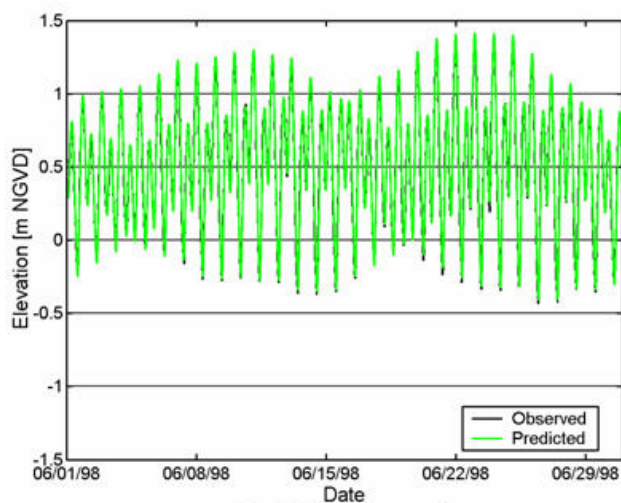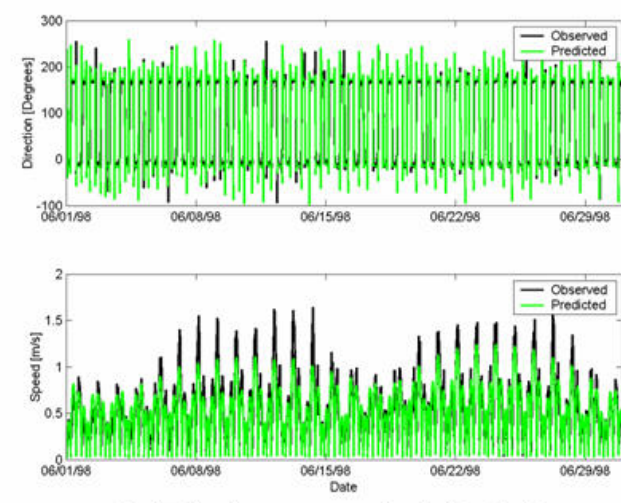
Figure 3 Observed and predicted water level at (a) San Francisco, (b) Point San Pablo, (c) Martinez, (d) Port Chicago, (e) Mallard, and current speed and direction at (f) Richmond ADCP.
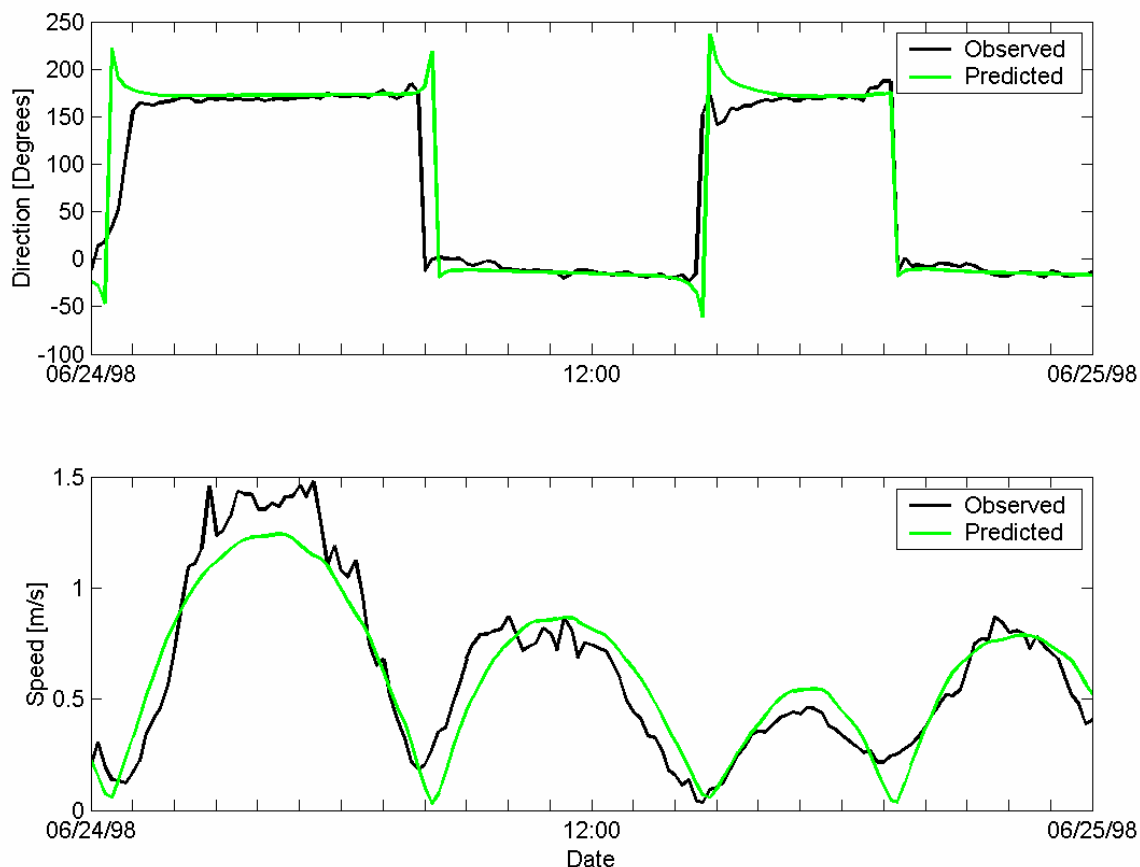
Figure 4 Observed and predicted current speed and direction at Richmond ADCP on June 24, 1998.

4.   MODEL VALIDATION

A validation period during 1980 was selected based on the availability of current meter data in San Pablo Bay. A 30-day period spanning from September 18 through October 18, 1980 was simulated. During this period, data from a total of two water level stations and seven current meter stations were available in or near San Pablo Bay, as shown on Figure 5. The sources and available data periods for the validation data set used in this study are shown in Table 2.

Predicted and observed water levels at Point San Pedro during the 1980 model validation period are shown on Figure 6a. The model slightly under predicts high water during the first few days of the analysis period and slightly under predicts low water on some days. However, overall the model shows equal to or better agreement with observed water levels at Point San Pedro than at Point San Pablo (the nearest water level station available during the calibration period) during the calibration period. Figure 6b shows predicted and observed water levels at Crockett, in Carquinez Strait, during the 1980 model validation period. Predicted water levels at Crocket show a similar trend to those at Point San Pedro with an under prediction of high water during the first few days of the analysis period and slightly under prediction of low water on some days. However, the level of agreement between predicted and observed water levels at Crockett is equal to or better than the level of agreement achieved at Martinez (the nearest water level station available during the calibration period) during the calibration period. These results suggest that the model calibration is robust and that water levels are equally well predicted using an independent data set.

Table 2 Model validation data sources.

| Location	Data Type	Data Source	Validation Record Length
Point San Pedro (9415009)	Water Level	NOAA	9/18/1980 – 10/18/1980
Crockett, Carquinez Strait (9415143)	Water Level	NOAA	9/18/1980 – 10/18/1980
C18	Mechanical Current Meter	Cheng and Gartner (1984)	9/25/1980 – 10/11/1980
C19	Mechanical Current Meter	Cheng and Gartner (1984)	9/17/1980 – 10/17/1980
C314	Mechanical Current Meter	Cheng and Gartner (1984)	10/9/1980 – 10/17/1980
C22	Mechanical Current Meter	Cheng and Gartner (1984)	9/18/1980 – 9/25/1980
C23	Mechanical Current Meter	Cheng and Gartner (1984)	9/30/1980 – 10/17/1980
C316	Mechanical Current Meter	Cheng and Gartner (1984)	10/6/1980 – 10/16/1980
C24	Mechanical Current Meter	Cheng and Gartner (1984)	9/18/1980 – 10/6/1980
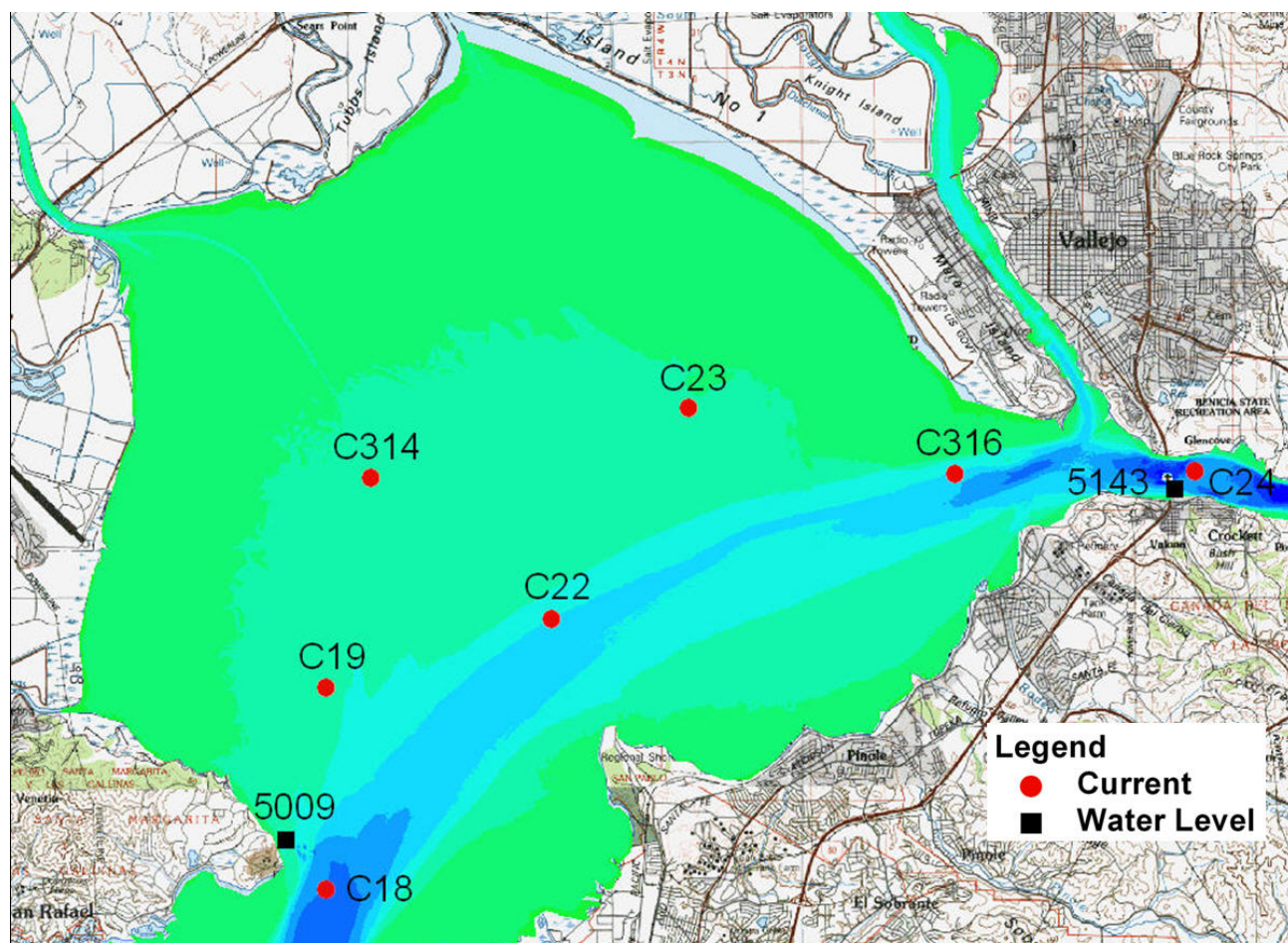
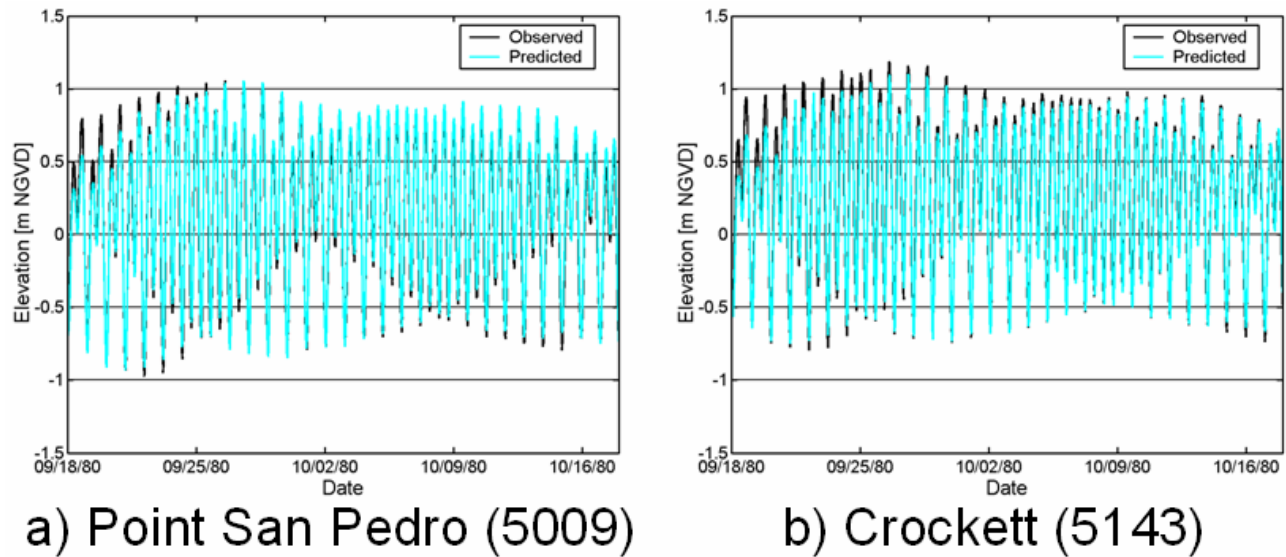Figure 5 Hydrodynamic data stations for the 1980 validation period.

Figure 6 Observed and predicted water levels at (a) Point San Pedro, and (b) Crockett during 1980 validation period.

An extensive current meter data set is available for San Pablo Bay during 1980. Mechanical current meters were deployed in San Pablo Bay as part of a larger study of tidal currents throughout San Francisco Bay (Cheng and Gartner, 1984; 1985). A total of seven current meter records are available during the 1980 validation period (Table 2). Each meter was deployed at a fixed depth above the bed. For comparison the predicted model velocity at the elevation where the mechanical meter was placed is plotted against the current velocity observed at that depth.

Predicted and observed current speed and direction at meter C18 is shown in Figure 7a. This station is located in fairly deep water and observed current speeds range from 0 to more than 1.5 m/s. The model under predicts velocity peaks on ebb tide, but accurately predicts the phase, direction, and the semi-diurnal pattern with the highest velocities occurring on ebb tides. This under prediction of peak ebb velocities is similar to the result seen for the nearby Richmond ADCP during the calibration period.

Figure 7b and Figure 7c show the predicted and observed current speed at meter C19 during the first half and second half of the observation period, respectively. Meter C19 is located in shallower water than meter C18, and the observed and predicted velocities range from 0 to approximately 0.6 m/s. The model slightly under predicts some velocity peaks on ebb tide, but accurately predicts the phase, direction, and the semi-diurnal pattern with the highest velocities occurring on ebb tides. The model also captures the spring-neap variability, with increasing current speeds and a decrease in semi-diurnal variability from September 17 to September 24. A reversed tend is evident on the predicted and observed velocities between October 8 and October 17 (Figure 7c) with a decrease in peak velocities but an increase in semi-diurnal variability. Meter C19 is the closest current meter to the proposed ATF sites in San Pablo Bay. The overall high level of agreement between predicted and observed current velocities at this station suggests that the model is accurately predicting current velocity distributions near the proposed project area.
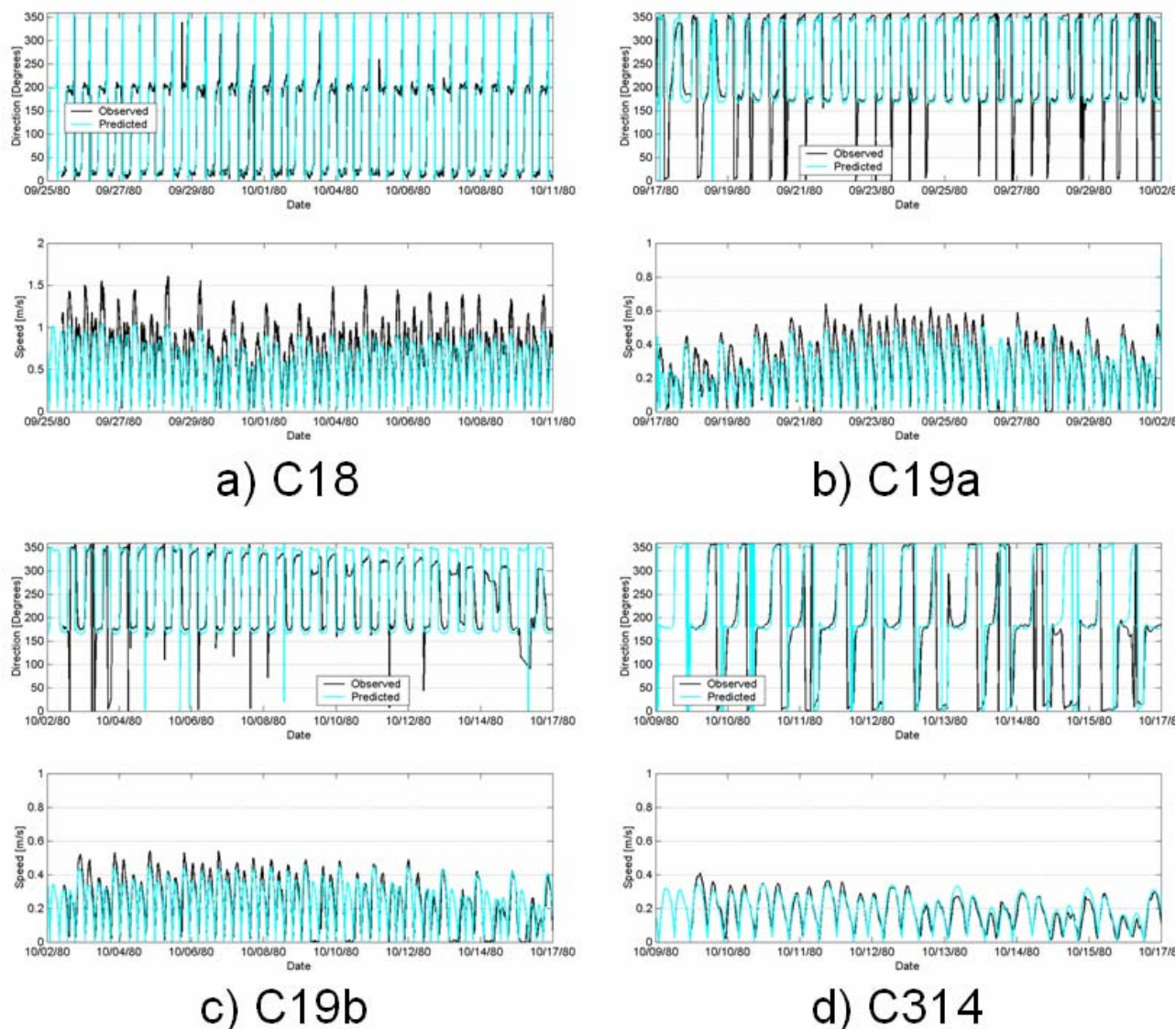
a) C18

b) C19a

c) C19b

d) C314

Figure 7 Observed and predicted current speed and direction at current meters (a) C18, at C19 during the (b) first half and (c) second half of the validation period, and at (d) C314.

Figure 7d shows the predicted and observed current speed and direction at meter C314. This station is located in shallower water and the predicted and observed current velocities range from 0 to 0.4 m/s. At meter C314, the model accurately predicts the speed, phase, direction, and the semi-diurnal pattern. Both the predicted and observed velocities show significantly less spring-neap variability at this meter than at the meters located in deeper water.

Predicted and observed current speed and direction at meter C22 is shown in Figure 8a. This meter is located in deeper water near the edge of the channel at the center of San Pablo Bay. Both predicted and observed current speeds range from 0 to almost 1 m/s, and are in good agreement. The model accurately predicts the speed, phase, direction, and the semi-diurnal pattern at this station. The difference in observed and predicted direction on September 18 and 19 during fairly weak current speeds highlights an inherent issue with mechanical current meters. During weak currents, the current is not always strong enough to fully turn and line-up the mechanical meter with the direction of the flow. As a result, the differences in direction seen on these two days are more
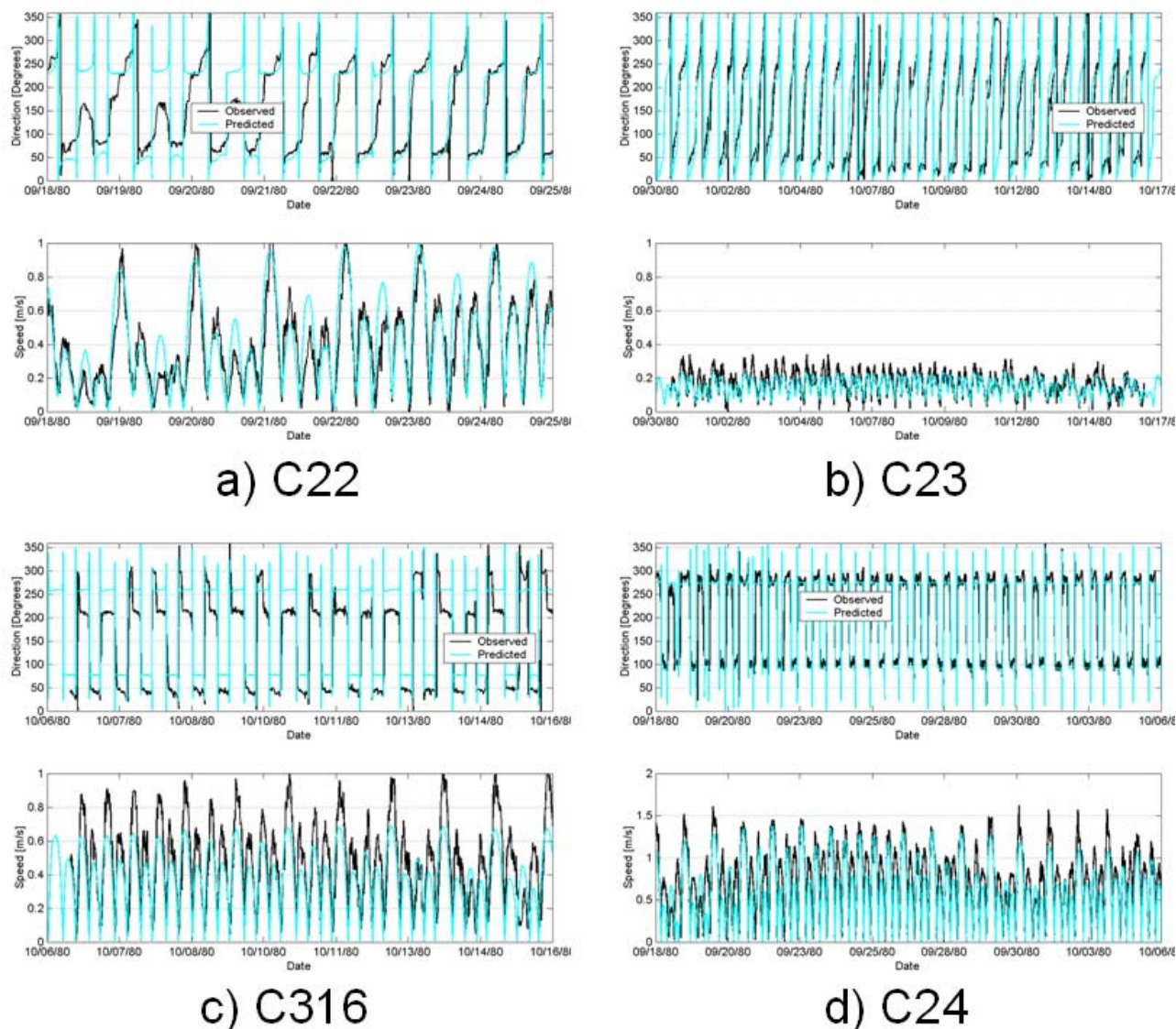
Figure 8 Observed and predicted current speed and direction at current meters (a) C22, (b) C23, (c) C316, and (d) C24.

likely to be attributed to an incorrect direction reading from the mechanical meter rather than an error in the predicted current direction from the model.

Figure 8b shows the observed and predicted current speed at meter C23. This meter is located in shallow water, where both observed and predicted current speeds range from 0 to less than 0.4 m/s. The model accurately predicts the speed, phase, direction, and the semi-diurnal pattern at this station. As with the meter C314, this meter shows very little spring-neap variability and exhibits a somewhat different semi-diurnal pattern in current speeds. The predicted current speeds accurately match both of these features.

Predicted and observed current speed and direction at meter C316 is shown in Figure 8c. This station is located in the channel near the entrance to Carquinez Strait, and observed current velocities range from 0 to almost 1 m/s. The predicted current direction shows some systematic differences to the observed direction. This may result from a slightly different placement in the model than the actual observation point (due to the precision of the reported instrument location). This meter is located in a region of rapidly varying bathymetry and fairly close to a large jetty that

extends into San Pablo Bay so the current speed and direction are likely to be very sensitive to small differences in the location at this site. The predicted velocities show a similar semi-diurnal pattern as observed velocities, but the model tends to under predict current speeds slightly throughout the data period.

Figure 8d shows the observed and predicted current speed at meter C24. This meter is located in fairly deep water in Carquinez Strait, and observed and predicted current speeds range from 0 to 1.5 m/s. The model accurately predicts the speed, phase, direction, and the semi-diurnal pattern at this station. This station, like the other deep-water stations shows a strong spring-neap variability that is also evident in the predicted velocities.

The comparison of the observed and predicted current speed and direction at these sites demonstrates that the model is accurately predicting current velocities over a wide range of depths and a large spatial extent. The model accurately predicts semi-diurnal variability of current speed and also captures the systematic differences in spring-neap variability evident between the observed velocities at the deeper and shallower meters.

5. DISCUSSION OF EXISTING CONDITIONS

This section presents an overview of the existing velocity and shear stress distribution in San Pablo Bay over the tidal cycle. The predicted depth-averaged velocity at each of the beginning and peak of flood and ebb tides, as well as the corresponding bed shear stress distribution calculated from the near bed velocity gives a good measure of the range of hydrodynamic conditions in San Pablo Bay during each tidal cycle. For this analysis, the model predictions for June 24, 1998, a day with relatively strong spring tides was selected. Observed and predicted current speed and direction at the Richmond ADCP were shown for this day in Figure 4.

5.1 Velocity

Figure 9 shows the depth-averaged velocity field in San Pablo Bay at the beginning of an ebb tide, the peak of an ebb tide, the beginning of a flood tide, and the peak of a flood tide on June 24, 1998. The start of the ebb tide was determined based on the velocity field in the vicinity of the project area (see Figure 1). Figure 9 shows both the depth-averaged velocity field over the entire area of San Pablo Bay, as well as depth-averaged current direction vectors at a uniform horizontal spacing, where the length of each vector is scaled to the local current speed. At the start of the ebb tide, the velocity is less than 0.5 m/s in most of San Pablo Bay, with somewhat higher velocities exiting San Pablo Bay into Carquinez Strait (where strictly the tide is still flooding) and in the southwest portion of San Pablo Bay (Point San Pablo) where ebb currents are already strong. Three hours later at the peak of ebb tide the highest velocities are in the channel, with depth-averaged velocities exceeding 1.5 m/s in some areas. Depth-averaged velocity on the shoals tends to be significantly lower than in the channel. At the start of flood tide, the velocity is less than 0.5 m/s in most of San Pablo Bay, with somewhat higher velocities entering San Pablo Bay through Carquinez Strait (where the primary current direction is still ebbing) and in the southwest portion of San Pablo Bay where flood currents are already stronger. Three hours later at the peak of flood tide the highest velocities are in the channel, with depth-averaged velocities exceeding 1.25 m/s in some areas. Depth-averaged velocity on the shoals tends to be significantly lower than in the channel. Properties of the velocity distribution are consistent with the peak velocities on ebb tides observed at the current meters in San Pablo Bay presented in Section 3.
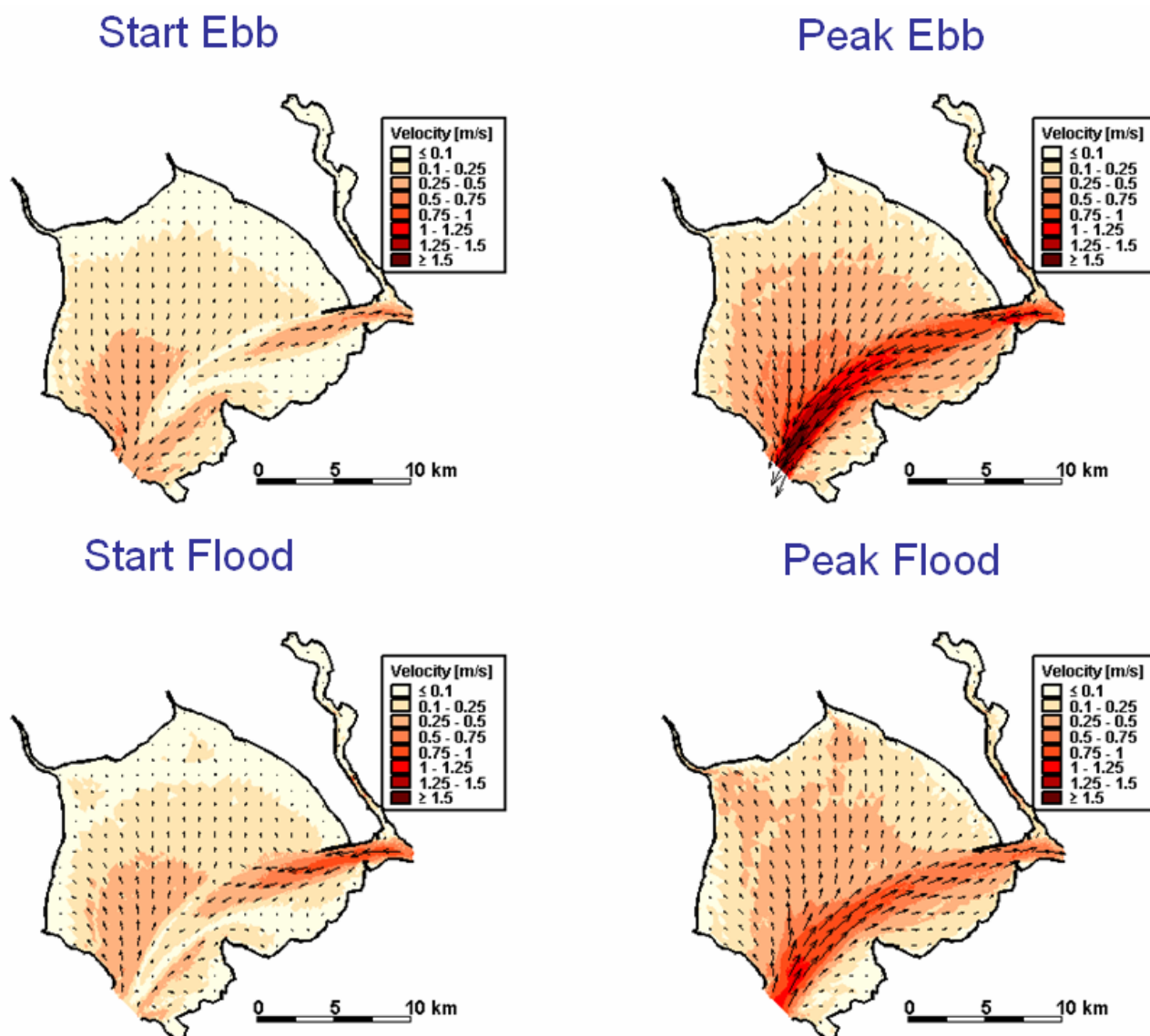
Figure 9 Predicted depth-averaged velocity distribution in San Pablo Bay at start and peak of an ebb tide, and start and peak of a flood tide during the tidal cycle on June 24, 1998.

5.2 Shear Stress

Bed shear stress, which is the primary force acting to cause mobilization of bed sediments, can be calculated from the near-bed velocity by:

$$\tau = \rho C_d u_b{}^2 \tag{1}$$

where ρ is the density of water, C_d is the drag coefficient, and u_b is the near-bed velocity. For this analysis, the predicted velocity at 1 meter above the bed was used as the near-bed velocity to calculate the bed shear stress. The drag coefficient can be evaluated through a variety of methods. The spatial distribution of the drag coefficient can depend on local sediment properties, however only limited data are available in the project area to estimate the drag coefficient. For the shear stress analysis presented in this study, a typical value of 0.0025 was. This value is consistent with the sediment transport analysis conducted as part of the ATF Technical study (Sea Engineering, Inc., 2006). They found that a good estimate of the drag coefficient could be calculated as 2 times the

D_{50} of the sediment bed by the method of Kamphuis (1974). Based on the values of D_{50} of the sediment samples taken near the project area, a value of 0.0025 gives a reasonable estimate for the coefficient of drag.

The predicted bed shear stress calculated from the predicted velocity 1 m above the bed and a C_d value of 0.0025 at the start of an ebb, peak ebb, and the start of a flood and peak flood during the tidal cycle are shown on Figure 10. At the start of an ebb tide, the shear stress is fairly low in most of San Pablo Bay with values ranging from 0.25 to 0.5 N/m^2 over most of the shoal areas and slightly higher values in Carquinez Strait and in the southwest portions of San Pablo Bay. At the peak of ebb tide, predicted shear stresses exceed 1.5 N/m^2 in the main channel of San Pablo Bay, and shear stresses on the shoals range from 0.25 to more than 1 N/m^2. The shear stress distribution at the start of flood tide is similar to the start of ebb tide. At peak flood, shear stresses in the channel again exceed 1.5 N/m^2, however overall the shear stresses at peak flood are somewhat less that at peak ebb, demonstrating the ebb dominance in this system.
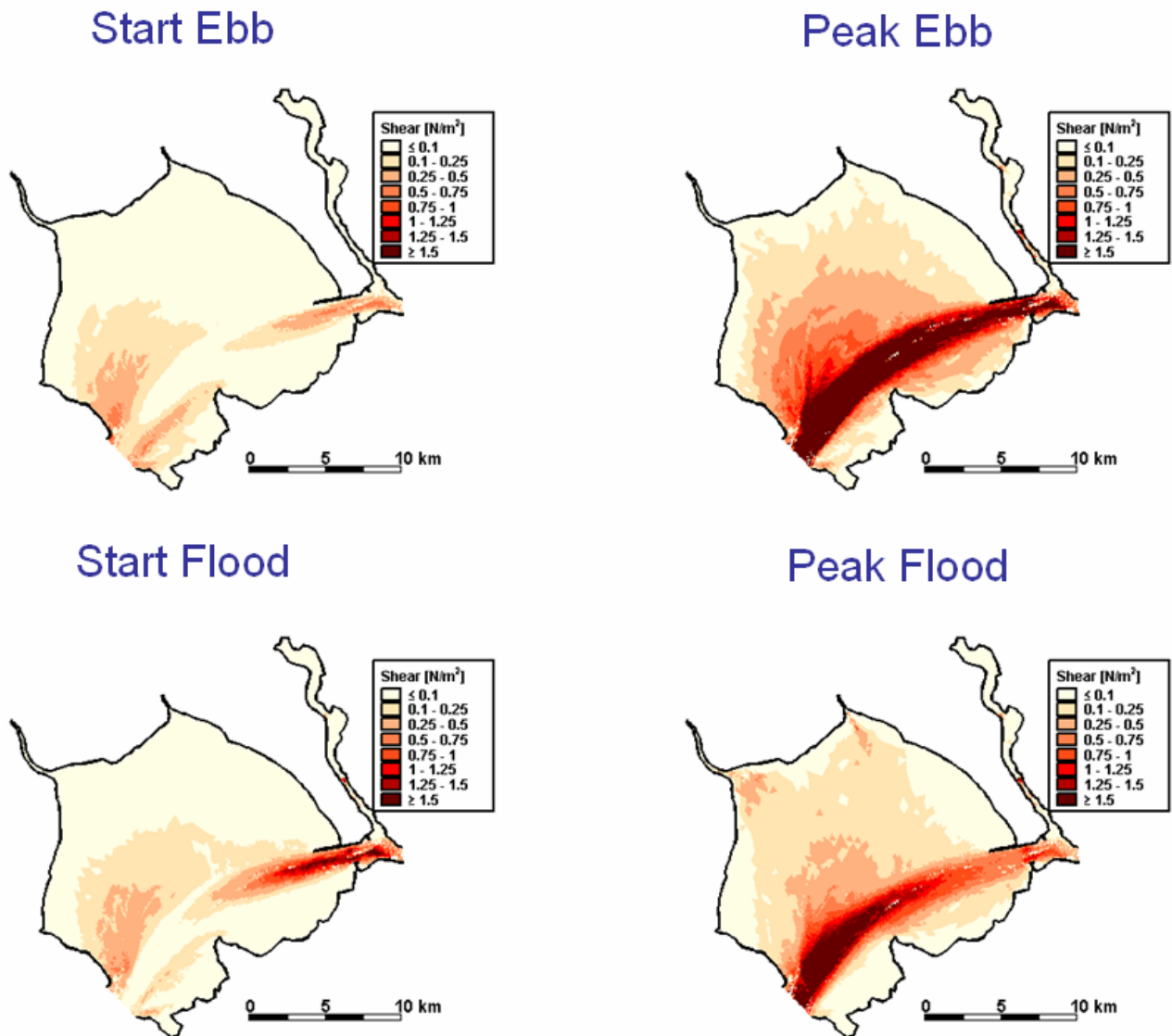

Figure 10 Predicted bed shear stress distribution in San Pablo Bay at start and peak of an ebb tide, and start and peak of a flood tide during the tidal cycle on June 24, 1998.

6.   CONCLUSIONS

A three-dimensional hydrodynamic model of San Francisco Bay was developed using the three-dimensional hydrodynamic model UnTRIM. The model was calibrated and validated using two independent data sets. The model was calibrated using continuous water level measurements and an ADCP data set collected during June of 1998. Water level comparisons were made over a one-month period at five continuous monitoring stations in Central, San Pablo, and Suisun Bay. The water level comparisons demonstrate that the model is accurately predicting tidal range and tidal propagation from the Pacific Ocean through Suisun Bay. Model validation was performed using water levels and extensive current velocity data collected in San Pablo Bay during 1980. The model calibration and validation using two independent data sets demonstrate that the San Francisco Bay model is accurately predicting water levels and tidal current velocity magnitude and direction in San Francisco Bay. In particular, the model has accurately predicted the extensive spatial distribution of current velocity measurements both in the channel and shoals in San Pablo Bay near the project area. The model results were used to evaluate the existing spatial and temporal velocity and shear stress distributions in San Pablo Bay over a tidal cycle. These results serve as the baseline conditions which were used to assess the potential impacts of the placement of an Aquatic Transfer Facility (ATF) in San Pablo Bay as part of the Hamilton Wetlands Restoration Project.

REFERENCES

Casulli, V. (1990). Semi-implicit finite difference methods for the two-dimensional shallow water equations. Journal of Computational Physics. 86, 56-74.

Casulli, V. and R. T. Cheng (1992). Semi-implicit finite difference methods for three-dimensional shallow water flow, Inter. J. for Numer. Methods in Fluids, Vol. 15, p. 629-648.

Casulli, V., and Cattani, E. (1994). Stability, accuracy and efficiency of a semi-implicit method for three-dimensional shallow water flow. Computers and Mathematics with Applications, 27(4), 99-112.

Casulli, V. (1999). A semi-implicit numerical method for non-hydrostatic free-surface flows on unstructured grid, in Numerical Modelling of Hydrodynamic Systems, ESF Workshop, pp. 175-193, Zaragoza, Spain.

Casulli, V. and R.A. Walters (2000). An unstructured, three-dimensional model based on the shallow water equations, International Journal for Numerical Methods in Fluids 2000, 32: 331 - 348.

Casulli, V. and Zanolli, P. (2002). Semi-Implicit Numerical Modelling of Non-Hydrostatic Free-Surface Flows for Environmental Problems, Mathematical and Computer Modelling, 36: 1131-1149.

Casulli, V. and Zanolli, P. (2005). High Resolution Methods for Multidimensional Advection-Diffusion Problems in Free-Surface Hydrodynamics, Ocean Modelling, 2005, v. 10, 1-2, p. 137-151.

Cheng, R.T. and Gartner, J.W. (1984). Tides tidal and residual currents in San Francisco Bay,

California, results of measurements, 1979-1980. Part III. Results of measurements in San Pablo Bay Region U. S. Geological Survey, Water Resources Investigations, Report 84-4339, 368 pp.

Cheng, R.T. and Gartner, J.W. (1985). Harmonic analysis of tides and tidal currents in South San Francisco Bay, California Estuarine, Coastal, and Shelf Science, Vol.21, p.57-74.

Cheng, R.T., Casulli, V., and Gartner, J.W. (1993). Tidal residual intertidal mudflat (TRIM) model and its applications to San Francisco Bay, California. Estuarine, Coastal and Shelf Science, 369, 235-280.

Cheng, R. T. and V. Casulli (1996). Modeling the Periodic Stratification and Gravitational Circulation in San Francisco Bay, in Proceedings of 4th Inter. Conf. on Estuarine and Coastal Modeling, Spaulding and Cheng (Eds.), ASCE, San Diego, CA, October 1995, p.240-254.

Cheng, R T. and R. E. Smith (1998). A Nowcast Model for Tides and Tidal Currents in San Francisco Bay, California, Ocean Community Conf. '98, Marine Technology Society, Baltimore, Nov. 15-19, p. 537-543.

Cheng, R. T., and V. Casulli (2002). Evaluation of the UnTRIM model for 3-D Tidal Circulation, Proceedings of the 7th International Conference on Estuarine and Coastal Modeling, St. Petersburg, FL, November 2001, 628-642.

Gross, E.S., Koseff, J.R., and Monismith, S.G. (1999). Three-dimensional salinity simulations of South San Francisco Bay. Journal of Hydraulic Engineering 125 (11), 1199-1209.

Gross ES, Schaaf & Wheeler (2003). South Bay Salt Ponds Initial Stewardship Plan: South San Francisco Bay Hydrodynamic Model Results Report. Prepared for Cargill Salt.

Gross, E. S., M. L. MacWilliams and W. Kimmerer (2006). Simulating Periodic Stratification in San Francisco Bay, Proceedings of the Estuarine and Coastal Modeling Conference, ASCE.

Kamphuis, J. W. (1974). Determination of sand roughness for fixed beds, Journal of Hydraulic Research, 12(2): 193-202.

SBSP (South Bay Salt Pond Restoration Project) (2006). http://www.southbayrestoration.org

Sea Engineering, Inc., (2006). Aquatic Transfer Facility Sediment Transport Analysis, prepared for U.S. Army Corps of Engineers San Francisco District, 25 pp.

Smith, R. E., Foxgrover, A., and P.E. Smith (2003). Suisun Bay & Delta Bathymetry: Production of a 10-meter Grid, http://sfbay.wr.usgs.gov/access/Bathy/Delta, Second Biennial CALFED Science Conference: Advances in Science and Restoration in the Bay, Delta and Watershed, Sacramento, California, January 14-16.

U.S. Army Corps of Engineers (USACE) (1988). Hamilton Army Airfield Wetland Restoration Feasibility Study. Prepared in Cooperation with the California State Coastal Conservancy. San Francisco District, San Francisco, December.